Dynamics of linear n-C-6-n-C-22 alkanes inside 5A zeolite studied by H-2 NMR

ARTICLE *in* THE JOURNAL OF PHYSICAL CHEMISTRY C · FEBRUARY 2007

Impact Factor: 4.77 · DOI: 10.1021/jp066959b

4 AUTHORS, INCLUDING:

Daniil Kolokolov
Boreskov Institute of Catalysis
28 PUBLICATIONS **305** CITATIONS
SEE PROFILE

Alexander G Stepanov
Boreskov Institute of Catalysis
136 PUBLICATIONS **1,674** CITATIONS
SEE PROFILE

Dynamics of Linear *n*-C_6−*n*-C_{22} Alkanes Inside 5A Zeolite Studied by ^{2}H NMR

Daniil I. Kolokolov,[†] Sergei S. Arzumanov,[‡] Alexander G. Stepanov,*[,†,‡] and Hervé Jobic*[,§]

Physical Department, Novosibirsk State University, Pirogova Street 2, Novosibirsk 630090, Russia, Boreskov Institute of Catalysis, Siberian Branch of the Russian Academy of Sciences, Prospekt Akademika Lavrentieva 5, Novosibirsk 630090, Russia, and Institut de Recherches sur la Catalyse, CNRS, 2 av. Albert Einstein, 69626 Villeurbanne, France

Received: October 24, 2006; In Final Form: December 19, 2006

The dynamic behavior of deuterated analogues of linear alkanes, *n*-C_6−*n*-C_{22}, adsorbed in zeolite 5A has been studied by deuterium solid-state NMR (^{2}H NMR). Temperature dependences of spin−lattice (T_1) and spin−spin (T_2) relaxation times of the deuterium located in the CD_3 groups of the adsorbed *n*-alkanes were rationalized on the basis of a model derived for the motion of *n*-alkanes located in the pores of the zeolite. The model implies that the adsorbed molecules consist of two ensembles: diffusing (or stretched) and temporarily blocked from diffusion (or coiled). The possible intramolecular motions for the alkane chains were taken into account based on both the finite size of the zeolite cage and the allowable hydrocarbon chain conformations. The coiled molecules are involved in two modes of motion: isotropic reorientation and intramolecular conformational isomerization, whereas the stretched molecules are additionally involved in a diffusion process. Dynamics parameters for different modes of motion and a proportion of the blocked and stretched molecules were derived from the analysis of relaxation data. The estimated proportion of the diffusing molecules correlates with the alkanes diffusivities earlier obtained by neutron spin echo measurements.

1. Introduction

In 1973, Gorring reported an experimental study of the diffusion of linear alkanes over zeolite T (an offretite/erionite intergrowth).[1] He found that the diffusivity decreased rapidly from ethane to propane, rising slightly for *n*-butane, and then dropping to a minimum at *n*-C_8. According to his results at 300 °C, the *n*-C_{12} molecule was moving through the zeolite lattice about 140 times faster than the *n*-C_8 molecule, and six times faster than propane, despite the difference in size. The high values of the diffusion coefficients in the *n*-C_{11} − *n*-C_{12} range relative to the lower values for *n*-C_8 and *n*-C_{14} indicated that the zeolite presented a "window of high transmittance" to molecules of a certain critical length, but not to those either shorter or longer. This phenomenon was designated as "window effect". The effect may be crucial for catalysis and separation. Indeed, Chen et al.[2] found that cracking of heavy alkanes in small pore zeolites such as erionite gave unusual product distribution, with maxima at approximately C_4 and C_{12} and a clear minimum at C_8. It was proposed that the product distribution in the cracking reaction was due to this anomalous transport phenomenon.[1] Since the experimental conditions of Gorring have been criticized, the reality of the window effect is a highly controversial issue.

Computer simulation studies have supported the possibility of window effect for *n*-C_6−*n*-C_{18} alkanes in erionite (ERI)[3] and chabazite (CHA)[3] zeolite structures, whereas anomalous increase of diffusivity was not detected for Linde type A zeolite.[4,5] The rationalization of window effect was as follows. The diffusivity increases by orders of magnitude when the molecular and cage shape are no longer commensurate, so a molecule ends up stretched across a cage tethered at opposite windows.[5] Computer simulations predicted that it could also occur for LTA-type sieves provided that the *n*-alkane is long enough (≥*n*-C_{23}) to exceed the diameter (1.1 nm) of the LTA α-cage.[3]

Recent neutron spin echo (NSE) measurement of *n*-C_6−*n*-C_{14} alkane diffusivities have clearly shown accelerated diffusion for *n*-C_{12} compared to *n*-C_8 and *n*-C_{14} alkanes in zeolite 5A.[6] The contradiction between experimental and theoretical results is evident. So, further studies are needed toward clarifying the window effect experimentally observed for 5A zeolite and to establish the interrelations among the dimension of the zeolite cage, the dimension of the window between the neighbor cages and the alkane molecule dimension. To shed some light upon the window effect exhibited by 5A zeolite and to resolve the discrepancy with molecular simulations, information on the rotational dynamics of alkanes occluded in the zeolite cages would be of great importance.

Deuterium solid-state NMR (^{2}H NMR) spectroscopy has been shown many times to be a powerful technique to probe the dynamics of alkanes[7−11] in zeolitic pores. ^{2}H NMR provides information on the peculiarities of the dynamics of both separate groups and the molecule as a whole for the adsorbed alkane, that is data which are complementary to PFG NMR,[12−15] QENS,[8,16−18] and theoretical MD simulations.[4,5,19−28] The line shape for ^{2}H NMR, being defined completely by intramolecular quadrupole interaction,[29−31] is especially sensitive to the nature of molecular motion and its rate.[30,31] Spin−lattice (T_1) and spin−spin (T_2) relaxation times bring also information on the energetics and the rate of the different intra- and intramolecular motions.

In the present paper, we report the results of ^{2}H NMR studies on the dynamic behavior of *n*-C_6−*n*-C_{22} alkanes inside 5A zeolite. Interpretation of the separate line shapes contributing

* Corresponding authors. Fax: +7 383 330 80 56. E-mail: stepanov@catalysis.ru. Fax: (33) 4 72 44 53 99. E-mail: herve.jobic@catalyze.cnrs.fr.
[†] Novosibirsk State University.
[‡] Boreskov Institute of Catalysis.
[§] Institut de Recherches sur la Catalyse.

10.1021/jp066959b CCC: $37.00
Published on Web 02/23/2007

to the total ^{2}H NMR spectrum of the adsorbed alkane and the temperature dependence of T_1 and T_2 relaxation times is made in terms of motional anisotropy, exhibited by the alkanes adsorbed in the zeolite.

2. Experimental Section

2.1. Materials. The sample of zeolite 5A was of commercial origin. It has 83% of Na^+ replaced by Ca^{2+} from starting NaA, and its chemical composition is $Na_{1.2}Ca_{5.4}Al_{12}Si_{12}O_{48}$. Perdeuterated alkanes, *n*-C_6−*n*-C_{22} with 98% ^{2}H isotopic enrichment were purchased from Cambridge Isotope Laboratories, Inc. and were used without further purification.

2.2. Samples Preparation. To prepare samples for the NMR experiments, approximately 0.3 g of 5A zeolite was loaded in a 5 mm (o.d.) glass tube, connected to a vacuum system. The sample was then heated at 670 K for 2 h in air and for 24 h under vacuum of 10^{-5} Torr (1 Torr = 133.3 Pa). After the sample was cooled back to room temperature, the zeolite was loaded with a certain amount of alkane and sealed off. The loading was 12 carbon atoms of any alkane per α-cage of the zeolite. It corresponded to 2 molecules of *n*-hexane, 1.5 molecules of *n*-octane, 1 molecule of *n*-dodecane, 0.67 molecules of *n*-octadecane per α-cage and so on. The adsorption was performed either from vapor or by a direct contact of a certain amount of the liquid or solid alkane under vacuum with the zeolite powder kept at the temperature of liquid nitrogen. The sealed sample was finally heated for 6−12 h at 423 K to obtain a uniform distribution of the adsorbed alkane over the zeolite sample. No quantity of *n*-C_6−*n*-C_{22} alkanes was detected on outer surface of the zeolite samples after long time heating at 423 K, as it followed from analyses of the ^{2}H NMR line shapes of corresponding alkanes.

2.3. NMR Measurements. ^{2}H NMR experiments were performed at 61.432 MHz on a Bruker Avance-400 spectrometer, using a high power probe with 5 mm horizontal solenoid coil. All ^{2}H NMR spectra were obtained by Fourier transformation of the quadrature detected quadrupole echo, arising in a pulse sequence[32,33]

$$\left(\frac{\pi}{2}\right)_{\pm X} - \tau_1 - \left(\frac{\pi}{2}\right)_Y - \tau_2 - \text{acquisition} - t \qquad \text{(i)}$$

where $\tau_1 = 30\ \mu$s, $\tau_2 = 34\ \mu$s, and t is a repetition time for the sequence (i) during the accumulation of NMR signal. The duration of the $\pi/2$ pulses was 3.0−4.5 μs. Spectra were typically obtained with 500−5000 scans and a repetition time of t = 0.4−2 s. Inversion−recovery experiments, to derive spin−lattice relaxation times (T_1), were carried out using the pulse sequence[34]

$$(\pi)_X - t_\nu - \left(\frac{\pi}{2}\right)_{\pm X} - \tau_1 - \left(\frac{\pi}{2}\right)_Y - \tau_2 - \text{acquisition} - t \qquad \text{(ii)}$$

where t_ν was a variable delay between the 180° $(\pi)_x$ inverting pulse (as in standard inversion−recovery pulse sequence[34]) and the quadrupole echo sequence (i). For the overlapping CD_3 and CD_2 signals of Lorentzian-type shape, contributing to the overall ^{2}H NMR line shape, T_1 values for CD_3 groups were calculated on the basis of the time τ_o ($\tau_o = 0.693\ T_1$). τ_o is the time t_ν for which the intensity of the NMR line changes from the inverted negative position to the normal positive one in the inversion−recovery experiment (sequence (ii)). τ_o (CD_3) was always notably higher than τ_o (CD_2). This allowed exact determination of T_1(CD_3). T_2 values for either CD_3 or CD_2 groups were derived from the Lorentzian-type spectra according to the well-known relation $T_2 = 1/\pi\Delta\nu_{1/2}$, where $\Delta\nu_{1/2}$ is the width at a half-height of the Lorentzian. T_2 for the CD_3 was derived at $t_\nu = \tau_o$, when the intensity of the CD_2 groups was equal to zero at spectrum acquisition with the sequence (ii), whereas T_2 for the CD_2 groups could be derived at $t_\nu = \tau_o$ with zero contribution to the NMR signal from the methyl groups. T_1 values were measured with accuracy 5−8%, whereas the estimation of the accuracy of T_2 values gave 7−10% interval with regard to the measured values.

The temperature of the samples was controlled with a flow of nitrogen gas, stabilized with a variable-temperature unit (Bruker model B−VT-3000) with a precision of ∼1 K; the sample was allowed to equilibrate at least 15 min at a given temperature before the NMR signal was acquired.

3. Theoretical Background

NMR Spectra. For deuterated alkanes, ^{2}H NMR spectra with nuclear spin $I = 1$ are entirely determined by the quadrupolar interaction that is by the interaction of the nuclear electric quadrupole moment **Q** with the electric-field gradient (EFG) tensor at the nuclear site.[29] The EFG tensor at the deuterium site of a hydrogen−carbon bond is assumed to be axially symmetric[35,36] with its principal axis component value $V_{zz} = q$ lying along the C−D bond direction and asymmetry parameter η close to zero. In this case, ^{2}H NMR spectra and relaxation times for deuterated alkanes are determined by the coupling constant $Q_0 = e^2Qq/h$ and by the type and the rate by which the C−D bond of the alkane orientationally moves in space.[35,37,38]

For molecules, which are rigid on the ^{2}H NMR time scale, i.e., when $\tau_{NMR} = Q_0^{-1} \sim 6 \times 10^{-6}$s [39] and the correlation times τ_C for molecular reorientation and internal motions satisfy the condition $\tau_C \gg \tau_{NMR}$, ^{2}H NMR spectra represent Pake-type powder patterns.[30,31] The dominant features of these line shapes are two strong peaks separated by the splitting $(3/4)Q_0 \approx 120$ kHz and two shoulders separated by $(3/2)Q_0$, $\eta \approx 0$ (see, e.g., Figure 1A in ref 8). If a CD_3 group of an alkane molecule undergoes fast threefold jumps or diffusion rotation about the C−CD_3 bond with a correlation time $\tau_P \ll \tau_{NMR}$, i.e., $\tau_P < 10^{-6}$−10^{-7} s and if isotropic reorientation of the molecule as a whole is slow ($\tau_R \gg \tau_{NMR}$), then the line shape of the spectrum for CD_3 groups will be similar to that of rigid molecules, but with the quadrupole splitting reduced to the value of $(3/4)Q_1$, $Q_1 = (1/3)Q_0$ (see, e.g., Figure 1B in ref 8).

When the correlation time τ_R for the isotropic reorientation of the molecule as a whole becomes comparable with τ_{NMR}, i.e., $\tau_R \sim \tau_{NMR}$, a broadening of the spectrum is observed and its sharp features are washed out.[39] For rapid isotropic reorientation as in liquids (i.e., when quadrupole splitting is averaged to zero), a single line of the Lorentzian shape is observed at ω_0, the Larmor frequency of the deuterium nucleus.

Relaxation Times. While spectral data provide us the information about interaction energy and allow qualitative analysis of molecular motion, a more detailed and quantitative description of the molecular motion can be obtained from an analysis of spin−lattice (T_1) and spin−spin (T_2) relaxation times data. The general expressions for T_1 and T_2 in case of nuclear spin $I = 1$ are well-known[31]

$$\frac{1}{T_1} = \frac{3}{4}\pi^2 Q_0^{\,2}(J(\omega_0) + 4J(2\omega_0)) \qquad (1)$$

$$\frac{1}{T_2} = \frac{3}{8}\pi^2 Q_0^{\,2}(3J(0) + 5J(\omega_0) + 2J(2\omega_0)) \qquad (2)$$

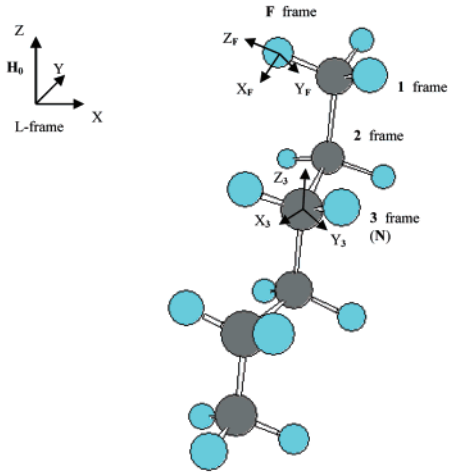

Figure 1. Schematic representation of the framework construction, used in the jump model formalism. The laboratory frame has its Z axis parallel to the static magnetic field H_o. Assuming there are N internal jump axes, frames 1 to N are chosen in such a manner that the Z axis of the i frame lies along the C_i−C_{i+1} bond; that is, the frame is attached to a proper carbon atom i. The final frame is attached to the deuterium atom of the CD_3 group and its Z axis is aligned with the C−D bond. It is possible to introduce a frame attached to the molecular center of the mass, however in our case we can combine it with the N frame.

Here $J(\omega)$ is the spectral density function. In our case, for quadrupolar interaction with $\eta = 0$, it is defined as

$$J(\omega) = 2\int_0^{\infty} \langle D^{(2)}_{q0}[\Omega_{NL}(0)]^* D^{(2)}_{q0}[\Omega_{NL}(t)]\rangle \cos \omega t \, dt \quad (3)$$

where $D_{q0}(\Omega_{NL}, t)$ are second-order Wigner rotation matrix elements[29,31] as a function of the Eulerian angle Ω_{NL} by which the transformation of the EFG tensor from its principal axis frame (N) into the laboratory frame (L) with the Z-axis in line with the Zeeman field is accomplished. In other words, the spectral density function is the Fourier transform of the autocorrelation function

$$g(t) = \langle D^{(2)}_{q0}[\Omega_{NL}(0)] D^{(2)}_{q0}[\Omega_{NL}(t)]\rangle \quad (4)$$

of the stochastic process responsible for the spin relaxation. As mentioned above, we consider that the main source of spin relaxation for deuterium NMR is the molecular motion.

In order to extract the exact information on the molecular motion from the experimental relaxation data we have to evaluate the spectral density and compare the obtained relaxation times with the experimental relaxation data. To evaluate spectral density we need to build an appropriate model for the molecular motion and then to calculate its autocorrelation function $g(t)$.

Model for the Motion of the Adsorbed Alkanes. Our experimental data consist of ^{2}H NMR spectra and relaxation times of deuterons located in methylene and methyl groups of n-alkanes. We are particularly interested in motional behavior of the terminal methyl groups since they are affected by all types of motions the molecule exhibits. Therefore, we completely specify the motion of the methyl groups. Figure 1 shows an example of how we define the reference frames for n-alkanes with the particular example for n-hexane. We consider that there are two independent types of molecular motions: the motion of the molecule as a whole and the motions of intramolecular origin. Such assumption makes it possible to simplify the general expression for the autocorrelation function

$$g(t) = \langle D^{(2)}_{q0}[\Omega_{LF}(0)] D^{(2)}_{q0}[\Omega_{LF}(t)]\rangle = \sum_{aa',bb'} \langle D^{(2)}_{qa}[\Omega_{LN}(0)] D^{(2)}_{qa'} [\Omega_{LN}(t)]\rangle \langle D^{(2)}_{b0}[\Omega_{NF}(0)]^* D^{(2)}_{b'0}[\Omega_{NF}(t)]\rangle \quad (5)$$

Here Ω_{LF} is Eulerian angle connecting the laboratory frame (L-frame) and the final frame (F-frame) attached to the deuterium, Ω_{LN} is the angle connecting the L-frame and the center of mass frame, combined with the molecular frame N, and the Ω_{NF} gives the orientation of the frame N in the frame F (see Figure 1).

Motion of the Molecule as a Whole. We consider two possibilities: rotational diffusion over the center of mass and translational diffusion via jumps of the molecule between zeolite cages. Rotational diffusion is considered to be isotropic due to the spherical symmetry of the molecule. This assumption needs a more detailed rationalization: although linear alkanes do not have such symmetry in a rigid state, the typical rates of their intramolecular motion (conformational isomerization) is much larger ($k_{intra} \sim 10^9$−10^{12} s^{-1})[8,40−43] than the rate of rotational diffusion ($k_{rd} \sim 10^5$−10^7 s^{-1}).[40,42,43] Therefore, the effective geometry of the molecule is assumed to be averaged to a spherically symmetric one. Hence, all orientations of the center of mass frame relative to the N frame are equivalent and we are free to choose the more convenient one. The more rational way is to combine the center of the mass frame and the N frame.

The geometrical properties of the adsorbed molecules and of the zeolite pores are of the same magnitude.[3] Therefore, it is evident that we need to take into account the steric factors to clarify the molecule behavior inside the zeolite. The adsorbed molecules can be in two qualitatively different states: coiled in the zeolite cage and stretched between two or more cages (Figure 2). The possibility for isotropic rotational diffusion is evident for the coiled molecule. For the case of the alkane stretched between two cages, the definition of isotropic diffusion loses its sense, since the molecule has no sufficient space to freely move as a whole. However, the possibility for the relatively free motion of the molecules ends which protrude through the windows still remains. Small oscillation of the molecule ends and other small vibrations of the molecule as a whole are also possible. These last motions can give a contribution only when the rotational diffusion is slowed down or absent. For the sake of simplicity, we count them as isotropic motion of the molecule as a whole with an effective rate constant k_{iso}.

The autocorrelation function for isotropic rotational diffusion is well-known[31,40,44] to be

$$g_R(t) = \frac{1}{5} e^{-t/\tau_R} \quad (6)$$

where τ_R is the correlation time of this motion.

Translational diffusion via jumps of the molecule between zeolite cages is also considered to be isotropic and its autocorrelation function is taken analogous to the well-known Brownian motion

$$g_D(t) = e^{-t/\tau_D} \quad (7)$$

where τ_D is the correlation time of this motion.

For the different states of the adsorbed molecules (Figure 2), we assume that there is a difference in allowed motions for coiled and stretched molecules. A coiled molecule is unable to jump to another cage until it becomes stretched. This is not

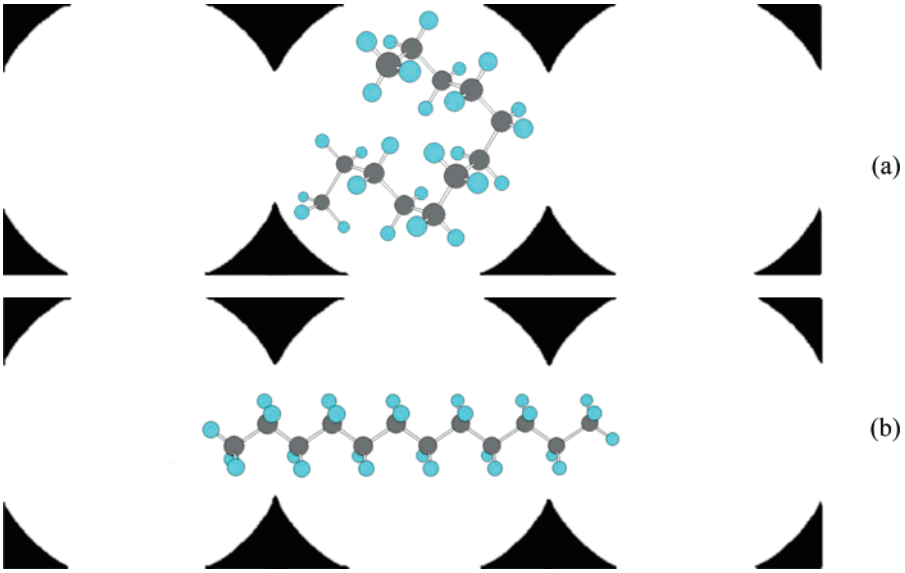

Figure 2. Schematic representation of a molecule of n-$C_{12}D_{26}$ inside the zeolite 5A: (a) a coiled one in the α-cage; (b) a stretched one among the α-cages.

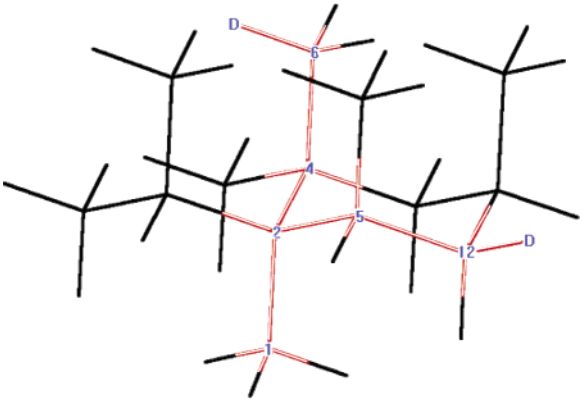

Figure 3. Two possible positions for a four carbon long alkane chain (1−2−4−6 and 1−2−5−12) on a tetrahedral lattice. Both positions define the allowed orientations of the C−D vector. In a given sample, in order to pass from one conformation to the another, the chain must execute two successive jumps over C−C bonds labeled as 2−5 and 1−2.

always possible due to geometrical factors: a finite volume of the zeolite cage and the presence of the neighboring molecules. Thus, we consider that all molecules within the zeolite pores are divided into two ensembles at every period of time: one of them consists of molecules diffusing among the cages and the second one consists of molecules coiled in the cages.

Intramolecular Motion. As it was proposed in ref 44, we represent the intramolecular motion as conformational isomerization. We assume that, in a coordinate system labeled N, the n-alkane chain can have M distinct conformations. We consider only half of the molecule chain since it is symmetrical relative to the center of mass. In each of these conformations the C−D vector, whose motion is responsible for the relaxation, has a certain known orientation and a probability of realization. The n-alkane chain is assumed to be restricted to lie on a tetrahedral lattice framework as suggested in ref 44 for conformational isomerization of the large paraffin chains in constrained areas (Figure 3). This assumption gives us the possibility to provide a more realistic description of the intramolecular motion of the adsorbed alkanes. By considering the steric factors of the zeolite and the excluded volume effect, we are able to select allowed conformation for each state of the adsorbed molecule (we mean here the coiled and the stretched states of the molecule).

A general autocorrelation function for such model is known as[44]

$$g_{\text{intra}}(t) = \langle D^*_{b0}(\Omega_{\text{NF}},0) D_{b'0}(\Omega_{\text{NF}},t)\rangle = \sum_{kl} D^*_{b0}(\Omega^l_{\text{NF}}) p_{\text{eq}}(l) D_{b'0}(\Omega^k_{\text{NF}}) p(\text{k},t|l,o) \quad (8)$$

where the sum goes over all conformations allowed. In other words $g_{\text{intra}}(t)$ is the autocorrelation function of the process of stochastic averaging of C−D vector orientation over all allowed conformations.

Equation 8 is one of the most important ones of this section and needs a more detailed clarification. The $D^*_{b0}(\Omega^l_{\text{NF}})$and $D_{b'0}(\Omega^k_{\text{NF}})$ values define the orientation of the C−D vector in the initial l and the resulting k conformations. $p_{\text{eq}}(l)$ is the equilibrium probability of the l conformation. $p(k,t\,|l,\,0)$ is the conditional probability that if the chain had conformation l at time $t = 0$ it will have conformation k at time t. In the rotational isomeric state approximation each conformation can be represented as a set of trans/gauche configurations. A gauche configuration is about 2 kJ mol^{-1} less stable that the trans one.[44] The equilibrium probability $p_{\text{eq}}(i)$ is proportional to $\exp(-2n_i/RT)$ where n_i is the number of gauche configurations in the i conformation. So the resulting equilibrium probability is

$$p_{\text{eq}}(i) = \frac{\exp\left(-\frac{2n_i}{RT}\right)}{\sum_{j=0}^{M} \exp\left(-\frac{2n_j}{RT}\right)} \quad (9)$$

The conditional probability (10) is the Green function of the master equation for the probability evolution

$$\frac{\partial p_i(t)}{\partial t} = \sum_{j=1}^{M} R_{ij} p_j(t)$$
$$p(k,t|l,0) = \exp(Rt)_{kl} \quad (10)$$

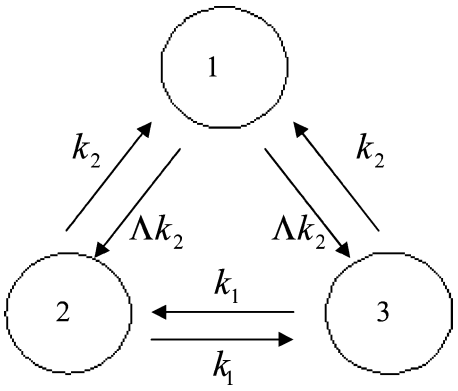

Figure 4. Schematic representation of a three site nonequally populated system. The model system has three possible conformations. To pass from the first to the second or to the third conformation, it has to perform 2 jumps over different C−C bonds. Only one jump is needed to pass from 2 to 3. The second and the third conformations have one additional gauche configuration as compared to the first conformation.

where R_{ij} is the rate constant for the transition from configuration j to i. Here we show how the rate matrix is built: the diagonal elements R_{ii} can be obtained from the expression $R_{ii} = -\sum_{j\neq i} R_{ij}$, this follows from its definition. Moreover, the R_{ij} satisfy the condition of microscopic reversibility

$$R_{ij}p_{eq}(j) = R_{ji}p_{eq}(i) \tag{11}$$

We consider that, to pass from the initial conformation of the molecule to the final one, the chain has to execute a number of jumps over distinct C−C bonds along the tetrahedral lattice. The rate constant for one elementary transition (i.e., for a single jump over one C−C bond) is taken to be k_1. The rate constant for two consecutive jumps is k_2; k_3 is the rate constant for three jumps, etc. If the final conformation k_1' is less energetically favorable than the initial one k_1, then the direct transition rate is lowered by the Boltzmann factor

$$k_1' = k_1 \exp\left(-\frac{(n_f - n_i)\epsilon}{RT}\right) \tag{12}$$

where n_f and n_i are the number of gauche configurations in the final and in the initial conformations, $\epsilon = 2$ kJ mol^{-1}.

For the sake of simplicity, we take the direct rate constant k_1 and its reverse value k_{-1} to be equal for conformations with equal number of gauche configurations. The same assumption is made for multiple jumps rate constants k_2, k_3, etc. The rate constants are defined by the Arrhenius law

$$k = k_0 \exp\left(-\frac{E_a}{RT}\right) \tag{13}$$

When the rate constants matrix is built, the orientation for each conformation is defined and all constants are determined; the autocorrelation function is constructed as shown in eq 5.

Figure 4 shows an example of how the rate matrix R is built for the system with three possible configurations in accordance to formalism originally described in ref 44. The rate constant matrix for such a system is[44]

$$R = \begin{pmatrix} -2\Lambda k_2 & \Lambda k_2 & \Lambda k_2 \\ k_2 & -k_2 - k_1 & k_1 \\ k_2 & k_1 & -k_2 - k_1 \end{pmatrix} \tag{14}$$

where $\Lambda = \exp(-\epsilon/RT)$.

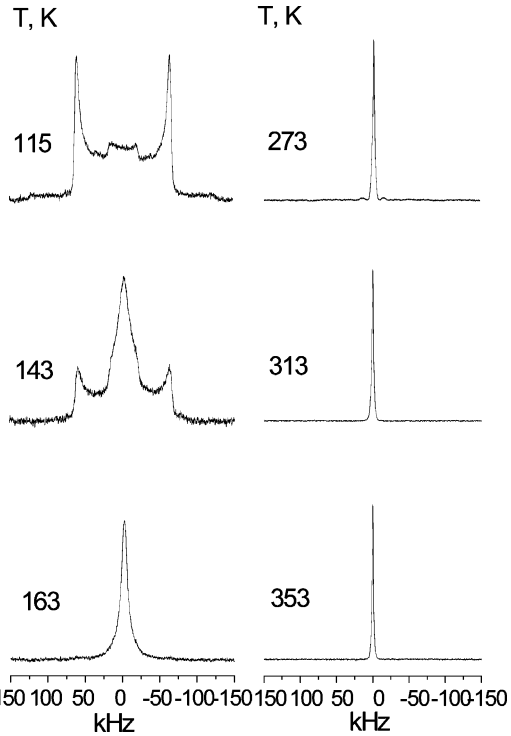

Figure 5. Typical temperature dependence of the ^{2}H NMR spectrum line shape of n-C_6-n-C_{22} alkanes adsorbed on zeolite 5A. An example for n-$C_{16}D_{34}$ is provided.

The resulting autocorrelation function for such simple systems is well-known[45] and can be easily evaluated. For relatively large systems as adsorbed long chain n-alkanes, it can only be obtained by numerical calculation. In our case, in order to evaluate the spectral density function for a certain temperature, one needs to enter the following parameters in eq 15: the set of rate constants k and the rate constant matrix for the system, which characterizes the motion, and then the set of orientations, a list of rotation matrices 5×5, which determine the orientation of each allowable conformation, and the list of equilibrium probabilities for each conformation

$$J(\omega) = \frac{2}{5}\sum_{l,k=1}^{N}\sum_{b=-2}^{2}\sum_{n=1}^{N} D_{b,0}^{l}(\Omega_l)^* D_{b,0}^{k}(\Omega_k) A_{l,n} \left(\frac{-(k_{iso} - \lambda_n)}{(k_{iso} - \lambda_n)^2 + \omega_I^2}\right) A_{n,k}^{-1} \tag{15}$$

Here $A_{l,n}$ is a matrix composed by eigen vectors of rate constant matrix R and λ_n are its eigen values and N is the total number of conformations.

4. Results and Discussion

^{2}H NMR Spectra. Figure 5 shows typical temperature dependence of ^{2}H NMR spectrum for the linear alkanes adsorbed on 5A zeolite. Each of the alkanes exhibits conditionally three different regions in the variation of the spectrum line shape with temperature. In the region of lowest temperatures (110−150 K), two signals are present. Both signals exhibit the Pake-powder line shapes. A broad signal with $(3/4)Q_0 = 126$ kHz belongs to immobile CD_2 groups of n-alkane,[38,46] whereas a narrow one with $(3/4)Q_1 = 42$ kHz, to the fast rotating CD_3 groups. In a second region (140−200 K), the narrow signal from CD_3 groups is averaged to the Lorentzian liquid-like line shape. The broad signal still remains anisotropic. The last region (170−400 K)

is characterized by a single isotropic line shape, composed of two signals from the CD_2 and CD_3 groups, different in their linewidths.

Such temperature dependences of the spectra line shapes demonstrate a consecutive change of the correlation time for the molecular motion.[29,31] In the first region, the isotropic motion of the molecule as a whole is reorienting the nuclear spins too slowly to average the anisotropic static spectra, and the correlation times for this motion are such that $\tau_R,\tau_D \gg \tau_{NMR}$. However, the methyl groups are less limited in their motion and they exhibit three sites jumps or free diffusion about $C-CD_3$ bond with the correlation time $\tau_P \ll \tau_{NMR}$. Hence, both signals exhibit the Pake-powder line shapes with different effective splitting constant. The second region corresponds to the growth of the rate of the isotropic motion, it becomes fast enough to average anisotropic signal of the CD_3 groups, $\tau_{NMR}/3 > \tau_R,\tau_D > \tau_{NMR}$. In the last region, the rate of isotropic motions further increases, $\tau_R,\tau_D \ll \tau_{NMR}$; both the CD_3 and CD_2 groups signals are averaged to liquid-like line shapes. The temperature dependence of the spectra line shapes offers us an important observation: the transition temperature to the isotropic spectral line shape is different for different alkanes.

Relaxation Times. Figure 6 show temperature dependence of the spin−lattice (T_1) and spin−spin (T_2) relaxation times for the methyl groups of the adsorbed *n*-alkanes in the temperature range where the spectra exhibit Lorentzian type line shape. The solid curves drawn through the data points are the theoretical fits according to the developed model of molecular motion for the specific *n*-alkanes. The model is discussed later on.

T_1 temperature dependences are typical for motion dependent NMR systems.[29,31] It is well-known that the main impact on T_1 is made by molecular motion with correlation time comparable with $\tau'_{NMR} = \omega_0^{-1} = 2.6 \times 10^{-9}$ s, ($\omega_0/2\pi = 61.43$ MHz). Some of the temperature dependences exhibit a well-defined minimum, which corresponds to the temperature where the correlation time for the fastest rotational motion of the molecule is comparable with $\tau'_{NMR} = \omega_0^{-1}$. Further growth of T_1 with the temperature increase is governed by the activation energy of the molecular motion. For some alkanes, local maxima are also distinct. They define the temperature where the intramolecular motions become too fast for T_1 to become more influenced by the isotropic motion, which is too slow at low temperature.

T_2 temperature dependences are more peculiar. T_2 is mainly governed by the slowest motion available; the main impact on T_2 is caused by motion with correlation time $\tau_C \sim \tau_{NMR} = 6 \times 10^{-6}$ s.[29,31] As can be seen from Figure 6 for *n*-$C_{14}D_{30}$, T_2 monotonically increases with the same slope at lowest and highest temperatures (i.e., with the same activation energy), but in the middle region, a short rapid growth interval is present. The change of T_2 slope with temperature can be rationalized by assuming that there are two ensembles of alkane molecules different by the characteristic time of isotropic reorientation. We assume one of the ensembles represents the molecules diffusing among the cages. The other one consists of molecules that are temporarily blocked from diffusion. The diffusing molecules are found in the stretched state, whereas the blocked molecules seem to be, at least partially, in a coiled state inside the zeolite cage. The coiled molecules can perform only isotropic reorientation inside the cages they already occupy, whereas the diffusing molecules can also isotropically move by the jumps among the zeolite cages. An extension of the T_2 rapid growth region is governed by the proportion of blocked molecules χ. The proportion χ can be directly estimated from T_2 temperature dependence. The ratio between these two ensembles is considered to be governed solely by geometrical factors of the zeolite framework and the adsorbed alkane molecules and to be temperature independent.

Table 1 offers the results of theoretical modeling of T_1 and T_2 temperature dependences. In this table, χ is the parameter that defines the amount coiled into the cages and non diffusing molecules: $N_{coiled} = \chi N_{total}$. E_{iso},k_{iso} and E_D,k_D are the activation energies and preexponential factors for isotropic rotation of the molecule as a whole and translational diffusion of the molecules among zeolite pores, respectively. k_1 and k_2 are rate constants for intramolecular motion (conformational isomerization) of the coiled molecules. As was described in a previous section, k_1 is the rate constant for conformational transition involving only one jump over the tetrahedral lattice. It is mainly influenced by the three site jump rate constant of the methyl groups. k_1 is the less affected by the sterical restrictions. k_2 is the averaged constant for conformational transition involving two or more jumps over the tetrahedral lattice. We assume k_2, k_3, etc. to be equal due to two reasons. First, introduction up to 5 rate constants for intramolecular motion makes our model too complicated for analysis. Second, it is clear from our spectral and T_1 data that our experimental method does not recognize multiple jumps over tetrahedral lattice as distinct motions. k'_1 and k'_2 are the rate constants for conformational isomerization for diffusing molecules. They can be significantly different from rate constants k_1 and k_2 for molecules in the coiled state as it will be seen further.

Motion of *n*-Hexane. Adsorbed *n*-hexane has 21 possible conformations. It completely fits the zeolite cage. There are no sterical restrictions for conformational isomerization. For the molecule which is in the ready-to-jump state (i.e., with its center of mass located in the window of α-cage the situation can be different): several conformations are now prohibited but the molecule can jump to the next cage. As a result, the contribution to the rate ($1/T_1$) of spin−lattice relaxation is formed by the two ensembles of molecules with slightly different values of the rate constants (see Table 1). The coiled molecules make contribution to the $1/T_1$ with the weight χ, and the diffusing ones with $1 - \chi$. However, due to the relatively small length of the alkane chain, the difference between the coiled and the diffusing molecules is small. The difference is displayed by the difference in rate constants of conformational isomerization, k_1 and k_2 and k'_1 and k'_2. In order to fit experimental data, we have to assume that the rate constant for isotropic rotation of the molecule as a whole is the same for both diffusing and blocked molecules. The same assumption is made for the other alkanes studied.

The specific behavior of the T_2 temperature dependence (Figure 6, *n*-C_6D_{14}) also follows directly from the model. As we already mentioned, T_2 relaxation time is mainly governed by the slowest type of motion available. The slowest motion should be the isotropic reorientation of the molecule as a whole. According to our model, the effective correlation time of isotropic reorientation for coiled molecules is governed by τ_{iso}, $\tau_{iso} = 1/k_{iso}$, where k_{iso} is the rate constant for isotropic rotation. An effective rate constant of isotropic reorientation for diffusing molecules is $k'_{iso} = k_{iso} + k_D$, $k_D = 1/\tau_D$. It is seen from Table 1 that the activation energy for rotational diffusion is several times lower than that for translational diffusion. For low temperatures $k_{iso} \gg k_D$, the effective constant k'_{iso} for the molecule reorientation as a whole is mainly governed by constant k_{iso}. As a result, two ensembles of molecules mentioned above have similar values of T_2, governed by k_{iso}.

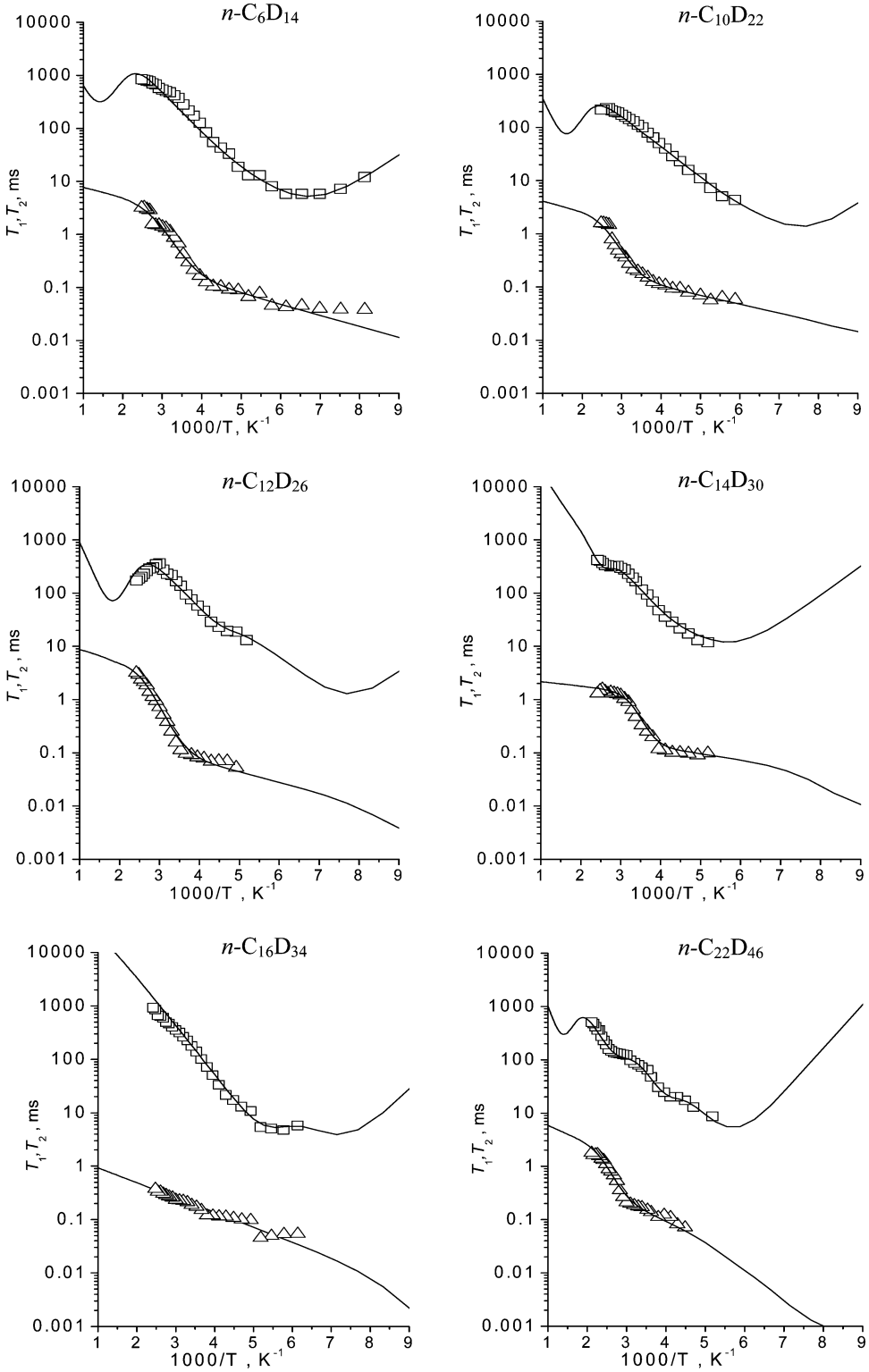

Figure 6. Temperature dependence of T_1 (□) and T_2 (△) for the methyl groups of n-C_6−n-C_{22} alkanes adsorbed on zeolite 5A. Solid curves represent fits to the experimental points on the basis of the developed model for molecular motion of the *n*-alkanes inside the zeolite pores. Six of nine obtained dependences are provided.

With increase of the temperature, k_D becomes comparable with k_{iso} and the diffusing molecules have an effective rate constant for the molecules reorientation as a whole k'_{iso} governed by the translational diffusion rate constant k_D. As a result, there is a rapid growth in the T_2 temperature dependence ($T >$ 250 K) with effective slope consisting of contributions from both coiled molecules ensemble (governed by k_{iso}) and the diffusing molecules ensemble (governed by k_D). As soon as the temperature increases enough for k_D to satisfy the condition $k_{iso} \ll k_D$, the diffusing molecules ensemble give no significant contribution to the T_2. T_2 is thus governed by the k_{iso} again ($T >$ 300 K). The region with T_2 rapid growth ($T =$ 250−300 K) is defined by the proportion of the diffusing molecules $1 - \chi$.

Motion of n-C_8−n-C_{22} Alkanes. *n*-Octane is the longest *n*-alkane that can fit into the zeolite pores in all-trans conformation. Though the number of conformations available is larger than for *n*-hexane, the molecule still fits the zeolite α-cages

TABLE 1: Dynamics Parameters for *n*-Akanes Adsorbed on the Zeolite 5A, Derived from Fitting the Experimental T_1 and T_2 Temperature Dependences, Based on the Proposed Model of the Adsorbed Alkane Motional Behavior

parameters[a]	n-C_6D_{14}	n-C_8D_{18}	n-$_{10}D_{22}$	n-$C_{12}D_{26}$	n-$C_{14}D_{30}$	n-$C_{16}D_{34}$	n-$C_{18}D_{38}$	n-$C_{20}D_{42}$	n-$C_{22}D_{46}$
χ[b]	0.06	0.3	0.14	0.05	0.15	0.85	0.2	0.2	0.17
E_{iso}, kJ mol^{-1}	2.5	4.7	3.1	3.65	1.0	4.8	5.8	5.3	5.0
$k_{0iso} \times 10^{-6}$, s^{-1}	0.8	6.5	2.4	2.2	0.18	1.9	2.5	2.2	2.1
E_D, kJ mol^{-1}	28[c]	42[c]	33	34.5[c]	43		33[c]	38	42
$k_{0D} \times 10^{-10}$, s^{-1}	7.1	560	35	120	300		40	6	70
E_1	10.5	10	12	19	9	7	4	22	26[d]
E_2, kJ mol^{-1}	15	13	13	18	18	17	24	22	26[d]
$k_{01} \times 10^{-10}$	5	50	160	900	30	70	700	50	390[d]
$k_{02} \times 10^{-10}$, s^{-1}	100	4	10	240	20	70	700	50	5[d]
E_1'	9	9	10.5	11.5	9.9	13	13	15	15
E_2', kJ mol^{-1}	15	3			15	13	13	17	15
$k_{01}' \times 10^{-10}$	20	580	310	950	9	340	110	1420	320
$k_{02}' \times 10^{-10}$, s^{-1}	300	4			80	340	110	120	120

[a]Errors in estimating the parameters are the following: $\chi \pm 0.005$, except for n-$C_{16}D_{34}$, where it is ± 0.10; $E_{iso} \pm 3-5\%$; $E_D \pm 10\%$; E_1, E_1', E_2, $E_2' \pm 5-7\%$; k_{01}, k_{02}, k_{01}', $k_{02}' \pm 10-20\%$. [b] χ is the parameter that defines the proportion of molecules temporarily blocked from diffusion. [c] Data from ref 6. [d] Corresponds to the average values of intramolecular motion for two dynamically different ensembles of the blocked molecules, see text.

and the difference of the properties of the intramolecular motion for the coiled and the diffusing molecules consists only of a small difference in the parameters of the motions (see Table 1).

n-Decane is the first of *n*-alkanes whose all-trans *c*onformation is not fitting the zeolite cage. It is the first molecule whose set of allowed conformations for the coiled and for diffusing states are different. We have assumed that both the coiled and the stretched molecules of n-C_6 and n-C_8 alkanes are symmetrical relative to the center of mass point. In the case of *n*-decane, in order to fit the experimental data, we have to assume that only a half of a molecule is found in a coiled state inside the cage. The second half of the molecule is coming out from one of the α-cage windows. The length of the end emergent into the next cage is equal to the length of one methyl group. The diffusing molecules are found to be stretched between two pore windows and the only intramolecular motion allowed are three site jumps about $C-CD_3$ bond. The activation energy of this motion for coiled and diffusing molecules is the same.

The *n*-dodecane behavior is almost the same as that for *n*-decane. The important difference lies in the intramolecular motion: the set of allowed conformations for coiled *n*-dodecane completely covers all of the space within the zeolite cage.

Although the model of molecular motion for *n*-tetradecane is similar to that of *n*-decane and *n*-dodecane, the emergent ends into the next pore for both coiled and diffusing molecules are represented by $CD_2-CD_2-CD_3$ segments.

The case of n-$C_{16}D_{34}$ is more complicated. There is no rapid growth in T_2 temperature dependence within a given temperature range, like there is, e.g., for *n*-hexane (Figure 6, n-$C_{16}D_{34}$). So, we were unable to determine the χ parameter from the T_2 dependence. A direct measurement of the diffusion of n-C_{16} performed by the NSE technique has shown that the diffusivity value is 1 order of magnitude smaller[47] than that of *n*-octane.[6] In other words, the diffusion rate constant for n-$C_{16}D_{34}$ should be essentially smaller in comparison with that for the other alkanes (Table 1). This means that k_D of n-C_{16} has no effect on the T_2 dependence. Another possibility to rationalize an absence of the bends on T_2 dependence for n-C_{16} is to assume that the proportion of diffusing molecules, $1 - \chi$, is too small to be reflected on the T_2 dependence.

The χ parameter can in principle be estimated from the T_1 temperature dependence, although with less accuracy. To define the parameter χ from such data, we need more detailed suggestions on the intramolecular motion for such a molecule. Let us assume that the molecule represents a stretched one across two α-cage windows in diffusing state. In such a situation, it occupies three cages and the molecule ends, emergent into the cage windows are as long as an *n*-butane molecule. A stretched molecule can also fit exactly in two pores as two *n*-octanes connected at the cage window. The blocked molecules can occupy two pores, but one of its ends is found in a coiled state. Taking into account a possible conformational isomerization of the molecules ends for both the coiled and the stretched molecules for such a model of the alkane location in the zeolite pores, analysis of T_1 dependences shows that the χ parameter should be 0.85.

n-$C_{18}D_{38}$ is longer and does not fit in all-*trans* configuration into two pores. The diffusing n-$C_{18}D_{38}$ molecules have the same activation energies for the intramolecular motion as diffusing n-$C_{16}D_{34}$ and the smaller alkane molecules (13 kJ mol^{-1}). The interaction with the zeolite framework increases with further growth of the molecules length. This results in an increase of the activation energies for intramolecular motion of the coiled molecules and for isotropic rotation of n-$C_{18}D_{38}$ (24 and 5.8 kJ mol^{-1}, respectively).

The n-$C_{20}D_{42}$ and n-$C_{22}D_{46}$ alkanes are similar in their motion to n-$C_{18}D_{38}$, and the influence of the translational diffusion on the T_2 temperature dependence is clearly seen (Figure 6, n-$C_{22}D_{46}$): a rapid growth interval is present. Although their internal motion can be described in the same way as it is for n-$C_{12}D_{26}$ and n-$C_{14}D_{30}$, the activation barriers defining this motion are close to the values for n-$C_{18}D_{38}$.

In the T_1 temperature dependence for the n-$C_{22}D_{46}$ alkane, two local minima can be clearly seen (Figure 6, n-$C_{22}D_{46}$). The motions that are responsible for them exhibit similar activation energies of 26 kJ mol^{-1}. The values of the activation energies point to the fact that these motions can correspond to the molecules in a coiled state. The only possibility to rationalize such a behavior is to suppose that for a certain reason, which has still to be defined, these coiled (blocked) molecules are additionally divided in two ensembles with different internal motion parameters. The preexponential factors and the activation energies for intramolecular motion of the coiled n-$C_{22}D_{46}$ (Table 1) define the average rate constants for two dynamically different ensembles. The numerical simulation shows that, with similar activation barriers, around 17% of blocked molecules have their ends moving about 100 times slower than the rest 83% of similar molecules.

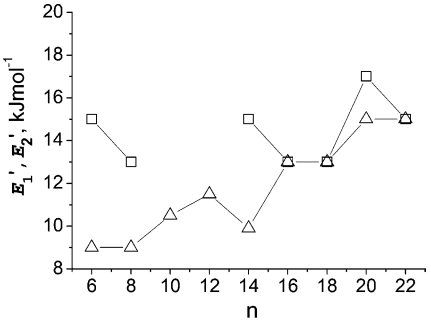

Figure 7. Dependence of activation energies E_1' (△) and E_2' (□) for intramolecular motion of the methyl groups on the chain length n for the stretched molecules.

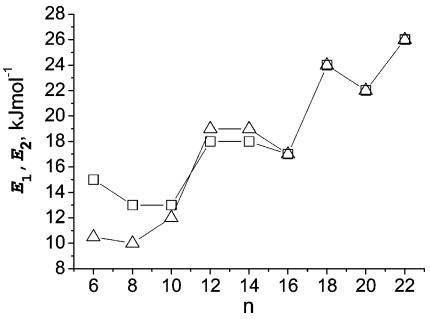

Figure 8. Dependence of activation energies E_1 (△) and E_2 (□) for intramolecular motion of the methyl groups on the chain length n for the coiled molecules.

Further Discussion. As we have shown (vide supra), the intramolecular motion of the adsorbed molecules is dependent on the length of the alkane. Not only are the allowed modes of motion different for coiled and stretched (diffusing) molecules but the parameters reflecting similar modes of motion are also different for the two ensembles of molecules. A better understanding of the influence of the cage constraints on intramolecular motion can give us the activation energies dependence of k_1 and k_2 on the *n*-alkane length.

As can be seen from Figures 7 and 8, for both the stretched and the coiled molecules whose length permits to fit easily into the zeolites pore (C_6−C_{10}), the activation energies for k_1' and k_2' and k_1 and k_2 have values close to those for corresponding motions in smaller *n*-alkanes (such as ethane or butane) in gas phase[48] with a small deviation within ∼2 kJ mol^{-1}. In fact, the activation energies for k_1' and k_1 (for C_6−C_{10}) have an average value of 11 ± 2 kJ mol^{-1}. This is very close to the activation energy for three site jumps of the methyl groups about C−C bond for *n*-alkanes in all-trans conformations (12.5 kJ mol^{-1}).[48] This indicates that these molecules are generally found in conformations which include no more than one gauche configuration and they are relatively free in their motion.

As can be seen from Figure 8, the activation energies of intramolecular motion for the coiled molecules can be divided into three groups. Alkanes in each group exhibit similar activation energies within a range of ±1 kJ mol^{-1}, whereas the difference between values for alkanes from different groups is equal to 3−5 kJ mol^{-1}. We can assume that this difference is related to the different package density of the coiled molecules of each group in the zeolite pores.

n-C_6−n-C_{10} alkanes, as was stated above, are able to fit into one pore with just one gauche configuration and the average activation energy for the internal motions (averaged over E_1' and E_2' and E_1 and E_2) is about 13 kJ mol^{-1}. n-C_{12}−n-C_{16} have to be coiled more tightly to fit the zeolite pore. At least two gauche configurations in the alkane chain are needed, and the barrier rises up to an average value of 18 kJ mol^{-1}. n-C_{18}, n-C_{20}, and n-C_{22} alkanes represent the next package; the activation energy for internal motions have the average value of 24 ± 2 kJ mol^{-1} at this package level. According to recent theoretical studies by Dubbeldam et al.[4] n-$C_{23}H_{48}$ is the longest *n*-alkane which could fit into the 5A zeolite pore. The maximum possible package density is predicted for this alkane. In this respect, further increase of the activation energy for internal motions with further growth of alkane chain is hardly possible.

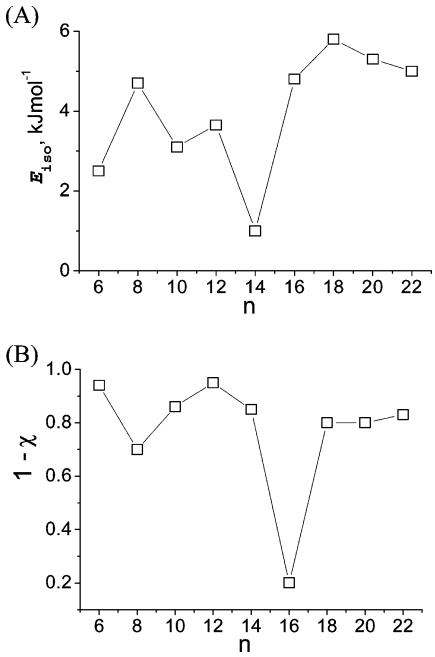

Figure 9. Dependences of activation energies E_{iso} for isotropic reorientation (A) and the proportion of the molecules in a diffusing state, 1 − χ, (B) on the *n*-alkane chain length *n*.

Therefore, it is clear from our data that the activation energy for intramolecular motion for the coiled molecules increases with the growth of the *n*-alkane chain and, therefore, with increase of package density and with the growth of alkane/zeolite and alkane/alkane interactions, governed by van der Waals interactions. Moreover, the activation energies for k_1 and k_2 are similar because they reflect intramolecular motions of the densely packed molecules. An averaged activation energy has the typical value of activation energies for conformational isomerization about the C−C bond for strongly sterically constrained conformations of *n*-alkanes configurations.[48]

The dependence of activation energy for isotropic reorientation on the alkane length is also quite informative for characterizing the state of the adsorbed alkanes in the zeolite (Figure 9 A). As was mentioned above, the origin of the activation barrier for isotropic rotation of the molecule as a whole arises from van der Waals interactions of the molecules with the zeolite framework inner structure. The more densely molecules are packed inside the zeolites pores the stronger the interaction with the zeolite framework is. Due to two ensembles of molecules present in the zeolite pores, the origin of the activation barrier for isotropic rotation is not trivial.

Now we consider the motion only for n-C_6D_{14}, n-C_8D_{18}, and n-$C_{16}D_{34}$ alkanes. *n*-Hexane has the smallest molecular length, and hence, it has the smallest activation barrier for isotropic reorientation, E_{iso}. The n-C_8D_{18} fits the pore in all-trans conformation, whose equilibrium probability is the largest among other conformations, and thus the molecule always directly interacts with the zeolite framework with both methyl groups. The n-$C_{16}D_{34}$ alkane fits only two pores and can be

roughly described as two *n*-C_8D_{18} molecules attached to each other through the window linking two α-cages, where both parts are located. Thus, close values of the activation barriers E_{iso} for *n*-C_8D_{18} and *n*-$C_{16}D_{34}$ are reasonable. A similar value of E_{iso} could be expected for *n*-$C_{24}D_{50}$, since we can describe it as three *n*-C_8D_{18} molecules occupying three subsequent α-cages.

The case of *n*-$C_{10}D_{22}$, *n*-$C_{12}D_{26}$, and *n*-$C_{14}D_{30}$ is more complicated. The experiment shows that E_{iso} decreases for these three alkanes, compared with *n*-C_8D_{18}. E_{iso} reaches its minimum for *n*-$C_{14}D_{30}$ and then rapidly rises for *n*-$C_{16}D_{34}$ as the difference between the coiled and stretched states becomes negligible. In principle, all studied alkanes can completely be packed into one zeolite cage. Therefore, it would be natural to assume that isotropic reorientation for the coiled molecules represents its rotation inside the zeolite cage. In this case, it would be expected that the longer the molecule, the more densely it is packed inside the cage, and the activation barrier should steadily increase with the alkane length. However, this model of isotropic reorientation cannot be valid for the diffusing molecules. These alkanes are stretched across the cage and can only have an effective isotropic motion of the molecule ends emergent into the neighboring cages. An activation barrier for isotropic reorientation should depend on the length of sticking out ends: the longer the end in a neighbour cage, the larger the activation barrier. The length of the sticking out ends seems to depend nonmonotonously on the total molecule length. This reflects nonmonotonous variation of E_{iso}. In order to achieve a qualitative agreement with experiment, we had to assume that the activation barriers of isotropic rotation for the coiled and diffusing molecules are similar. This isotropic reorientation for both the coiled and stretched alkanes can be performed in the following manner. The molecule larger than C_8 occupies at least two pores while isotropically reorienting. The molecule ends perform a similar isotropic rotation in their cages and the average activation barrier for their rotation depends on the length of each end. While isotropically reorienting, *n*-$C_{10}D_{22}$, *n*-$C_{12}D_{26}$, and *n*-$C_{14}D_{30}$ alkanes occupy two cages only partially, and *n*-$C_{16}D_{34}$ occupies exactly two pores. Although we cannot precisely define why *n*-$C_{14}D_{30}$ has a smaller activation barrier than *n*-$C_{12}D_{26}$ or *n*-$C_{10}D_{22}$, we can state that they have larger freedom for isotropic reorientation than the *n*-C_8D_{18} and the *n*-$C_{16}D_{34}$ alkanes and thus a smaller activation barrier for it.

For *n*-$C_{18}D_{38}$, *n*-$C_{20}D_{42}$, and *n*-$C_{22}D_{46}$ the activation barrier E_{iso} smoothly goes down to the level of ∼5 kJ mol^{-1} [i.e., to the level of *n*-$C_{16}D_{34}$ (see Figure 9A and Table 1)]. A simple way to understand such dependence is to picture the adsorbed molecules as a number of molecular chain segments connected through α-cages windows. Each segment occupies one α-cage. Because of the small size of the window, the influence of segments on each others intermolecular motion is damped. The activation barrier for isotropic rotation could depend on the strength of interaction of each segment with the inner surface of its pore. In other words, the activation energy for isotropic rotation may depend not only on motion of the segments with terminal methyl groups but also on the motion of the inner segments of the molecule. It is natural to expect that with growth of the alkanes length the inner segments will have a greater impact on isotropic reorientation than the terminal segments. In this regard, we expect the activation barrier for isotropic rotation to be around 5 kJ mol^{-1} and will not further increase for the alkanes longer than *n*-C_{22}.

Among all alkanes studied, *n*-$C_{12}D_{26}$ has the largest diffusion rate constant (see Figure 10) and therefore the highest translational mobility. We consider this fact to be an additional

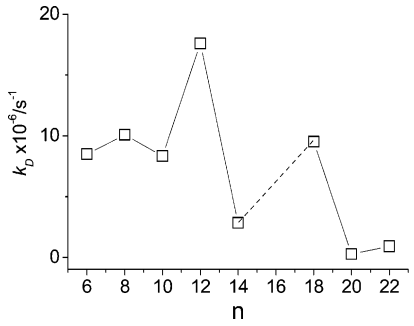

Figure 10. Dependence of the rate constant for diffusion k_D at 373 K on the *n*-alkane chain length *n*.

experimental evidence for accelerated diffusion of *n*-C_{12} reported in ref 6. We suppose that the prediction that the *n*-C_{23} alkane should show the maximum diffusion for LTA type zeolites made by Dubbeldam and Smit[5] could be a consequence of inaccuracy of the model used.

Another interesting result lies within the dependence of the parameter χ on the alkane length (Figure 9B). The dependence is reproducing the nonmonotonous dependence of the diffusivity of the *n*-alkanes adsorbed in the zeolite.[6] In this respect, the parameter χ can be used to qualitatively characterize the relative ability of the alkane to diffuse in the zeolite pores. The more the proportion of diffusing molecules, the faster the diffusivity is. Our experimental data indicates that the translational diffusion rate constant and the χ parameter for *n*-$C_{16}D_{34}$ are significantly lower in comparison with other *n*-alkanes studied. The same can be also noted for *n*-C_8D_{18} alkane. For alkanes with chain length multiple to the length of the *n*-octane, i.e., *n*-C_8D_{18}, *n*-$C_{16}D_{34}$, *n*-$C_{24}D_{50}$, and so on, the diffusion rate constant should be significantly lower in comparison to the neighboring alkanes.

5. Conclusion

Analysis of the temperature dependences of ^{2}H NMR T_1 and T_2 relaxation times for deuterated *n*-C_6−*n*-C_{22} alkanes adsorbed on zeolite 5A, based on a model proposed for the motions of the adsorbed *n*-alkanes, allowed us to draw the following conclusions on the peculiarities of the motional behavior of *n*-alkanes in the pores of the zeolite. The alkanes exist in two ensembles differentiated by their mobility: the coiled (or blocked) and diffusing (or stretched) molecules. The proportion of the diffusing molecules is defined by the size of the alkane and the geometrical dimensions of the zeolite cage. The isotropic reorientations of the coiled and diffusing molecules are similar and are performed within a time scale of a few microseconds at 300−370 K. Diffusion of the stretched molecules is performed within the time scale of 1 or 2 orders of magnitude larger compared with the isotropic reorientation time scale. Intramolecular reorientations of the adsorbed alkanes are performed within a time scale of 10^{-9}−10^{-11}s. The peculiarities of the alkanes intramolecular motions for the diffusing and the coiled molecules have been clearly distinguished. Intramolecular motion shows an average value of the activation energies E_1' and E_2' of 13 kJ mol^{-1} for the stretched molecules and does not change significantly with the chain length. Intramolecular motion exhibits strong dependence of E_1 and E_2 on the chain length for the coiled molecules. E_1 and E_2 increase consecutively from 13 to 26 kJ mol^{-1} for the *n*-C_6− *n*-C_{22} alkanes. This increase of E_1 and E_2 has been interpreted as an increase of the molecule package density and strengthening of the alkane/zeolite and alkane/alkane van der Waals interactions with the alkane chain increase. The estimated proportion of the diffusing molecules

correlates with the alkanes diffusivities earlier derived from neutron spin echo measurements.[6] Among all alkanes studied, n-$C_{12}D_{26}$ has the largest diffusion rate constant. We consider this fact to be additional experimental evidence for accelerated diffusion of *n*-dodecane in zeolite 5A, as reported in ref 6.

Acknowledgment. This work was performed in a frame of French-Russian Laboratory of Catalysis. The work was supported by the Russian Foundation for Basic Research (Grant No. 05−03-34762).

References and Notes

(1) Gorring, R. L. *J. Catal.* **1973**, *31*, 13.
(2) Chen, N. Y.; Lucki, S. J.; Mower, E. B. *J. Catal.* **1969**, *13*, 329.
(3) Baerlocher, C.; Meier, W. M.; Olson, D. H. *Atlas of Zeolite Framework Types*, 5th revised ed.; Elsevier: Amsterdam, 2001.
(4) Dubbeldam, D.; Calero, S.; Maesen, T. L. M.; Smit, B. *Phys. Rev. Lett.* **2003**, *90*, 245901.
(5) Dubbeldam, D.; Smit, B. *J. Phys. Chem. B* **2003**, *107*, 12138.
(6) Jobic, H.; Méthivier, A.; Ehlers, G.; Farago, B.; Haeussler, W. *Angew. Chem., Int. Ed.* **2004**, *43*, 364.
(7) Silbernagel, B. G.; Garcia, A. R.; Newsam, J. M.; Hulme, R. *J. Phys. Chem.* **1989**, *93*, 6506.
(8) Stepanov, A. G.; Shubin, A. A.; Luzgin, M. V.; Jobic, H.; Tuel, A. *J. Phys. Chem. B* **1998**, *102*, 10860.
(9) Sato, T.; Kunimori, K.; Hayashi, S. *Phys. Chem. Chem. Phys.* **1999**, *1*, 3839.
(10) Stepanov, A. G.; Shubin, A. A.; Luzgin, M. V.; Shegai, T. O.; Jobic, H. *J. Phys. Chem. B* **2003**, *107*, 7095.
(11) Stepanov, A. G.; Shegai, T. O.; Luzgin, M. V.; Jobic, H. *Eur. Phys. J. E* **2003**, *12*, 57.
(12) Heink, W.; Karger, J.; Pfeifer, H.; Stallmach, F. *J. Am. Chem. Soc.* **1990**, *112*, 2175.
(13) Karger, J.; Ruthven, D. M. *Diffusion in Zeolites and Other Microporous Solids*; Wiley-Interscience: New York, 1992**.**
(14) Heink, W.; Karger, J.; Ernst, S.; Weitkamp, J. *Zeolites* **1994**, *14*, 320.
(15) Karger, J.; Bar, N. K.; Heink, W.; Pfeifer, H.; Seiffert, G. *Z. Naturforsch. A* **1995**, *50*, 186.
(16) Jobic, H.; Bee, M.; Caro, J. Translational Mobility of n-Butane and n-Hexane in ZSM-5 Measured by Quasi-elastic neutron Scattering. In *Proceedings 9th International Zeolite Conference, Montreal, 1992*; von Ballmoos, R., Higgins, J. B., Treacy, M. M. J., Eds.; Butterworth-Heinemann: Boston, 1993; Vol. II, p 121.
(17) Jobic, H.; Bee, M. *Z. Phys. Chem.* **1995**, *189*, 179.
(18) Jobic, H. *Phys. Chem. Chem. Phys.* **1999**, *1*, 525.
(19) June, R. L.; Bell, A. T.; Theodorou, D. N. *J. Phys. Chem.* **1990**, *94*, 1508.
(20) Catlow, C. R. A.; Freeman, C. M.; Vessal, B.; Tomlinson, S. M.; Leslie, M. *J. Chem. Soc. Faraday Trans.* **1991**, *87*, 1947.
(21) June, R. L.; Bell, A. T.; Theodorou, D. N. *J. Phys. Chem.* **1992**, *96*, 1051.
(22) Smit, B.; Siepmann, J. I. *J. Phys. Chem.* **1994**, *98*, 8442.
(23) Maginn, E. J.; Bell, A. T.; Theodorou, D. N. *J. Phys. Chem.* **1996**, *100*, 7155.
(24) Runnebaum, R. C.; Maginn, E. J. *J. Phys. Chem. B* **1997**, *101*, 6394.
(25) Webb, E. B., III;, Grest, G. S. *Catal. Lett.* **1998**, *56*, 95.
(26) Webb, E. B., III;, Grest, G. S.; Mondello, M. *J. Phys. Chem. B* **1999**, *103*, 4949.
(27) Bouyermaouen, A.; Bellemans, A. *J. Chem. Phys.* **1998**, *108*, 2170.
(28) Clark, L. A.; Ye, G. T.; Gupta, A.; Hall, L. L.; Snurr, R. Q. *J. Chem. Phys.* **1999**, *111*, 1209.
(29) Abragam, A. *The Principles of Nuclear Magnetism*; Oxford University Press: Oxford, 1961.
(30) Mehring, M. Principles of High Resolution NMR in Solids. In *NMR Basic Principles and progress*; Diehl, P., Fluck, E., Kosfeld, R., Eds.; Springer-Verlag: New York, 1976; Vol. 11.
(31) Spiess, H. W. Rotation of Molecules and Nuclear Spin Relaxation. In *NMR Basic Principles and Progress*; Diehl, P., Fluck, E., Kosfeld, R., Eds.; Springer-Verlag: New York, 1978; Vol. 15, p 55.
(32) Powles, J. G.; Strange, J. H. *Proc. Phys. Soc.* **1963**, *82*, 6.
(33) Davis, J. H.; Jeffery, K. R.; Bloom, M.; Valic, M. I.; Higgs, T. P. *Chem. Phys. Lett.* **1976**, *42*, 390.
(34) Farrar, T. C.; Becker, E. D. *Pulse and Fourier Transform NMR. Introduction to Theory and Methods*; Academic Press: New York, 1971.
(35) Barnes, R. G. *Adv. Nucl. Quadrupole Reson.* **1974**, *1*, 335.
(36) Mantsch, H. H.; Saito, H.; Smith, I. C. P. *Progr. Nucl. Magn. Reson. Spectrosc.* **1977**, *11*, 211.
(37) Spiess, H. W. In *Dynamic NMR Spectroscopy*; Springer-Verlag: Berlin, 1978; Vol. 15, p 55.
(38) Jelinski, L. W. Deuterium NMR of Solid Polymers. In *High Resolution NMR Spectroscopy of Synthetic Polymers in Bulk (Methods and Stereochemical Analysis*); Komoroski, R. A., Ed.; VCH Publishers: New York, 1986; Vol. 7, p 335.
(39) Stocktone, G. W.; Polnaszek, C. F.; Tulloch, A. P.; Hasan, F.; Smith, I. C. P. *Biochemistry* **1976**, *15*, 954.
(40) Boddenberg, B.; Beerwerth, B. *J. Phys. Chem.* **1989**, *93*, 1440.
(41) Burmeister, R.; Boddenberg, B.; Verfurden, M. *Zeolites* **1989**, *9*, 318.
(42) Meirovitch, E.; Rananavare, S. B.; Freed, J. H. *J. Phys. Chem.* **1987**, *91*, 5014.
(43) Schwartz, L. J.; Meirovitch, E.; Ripmeester, J. A.; Freed, J. H. *J. Phys. Chem.* **1983**, *87*, 4453.
(44) Wittebort, R. J.; Szabo, A. *J. Chem. Phys.* **1978**, *69*, 1722.
(45) Torchia, D. A.; Szabo, A. *J. Magn. Reson.* **1982**, *49*, 107.
(46) Rinne, M.; Depireux, J. *Adv. Nucl. Quadrupole Reson.* **1974**, *1*, 357.
(47) NSE experiment has shown a diffusion coefficient of 1×10^{-13} m^2 s^{-1} for n-$C_{16}H_{34}$ at 475 K.
(48) Morrison, R. T.; Boyd, R. N. *Organic Chemistry*; Allyn & Bacon, Inc.: Boston, 1970.